Proc. of the International Conference on Mechanochemistry and Mechanical Alloying, Kraków, Poland, June 22–26, 2014

Physico-Chemical and Biological Properties of Arsenic Sulfide ($As_{55}S_{45}$) Nanosuspension Prepared by Milling

Z. Bujňáková[a,*], O. Shpotyuk[b,c], J. Sedlák[d], M. Pastorek[d], E. Turianicová[a], P. Baláž[a] and A. Ingram[e]

[a]Institute of Geotechnics, Slovak Academy of Sciences, Watsonova 45, 04001 Košice, Slovakia
[b]Scientific Research Company "Carat", 202, Stryjska Str., Lviv, 79031, Ukraine
[c]Institute of Physics, Jan Długosz University, al. Armii Krajowej 13/15, 42-200 Częstochowa, Poland
[d]Cancer Research Institute, Slovak Academy of Sciences, 7, Vlárska Str., Bratislava, 83391 Slovakia
[e]Opole University of Technology, Ozimska 75, 45-370 Opole, Poland

Nanosuspension based on melt-quenched arsenic sulfide of nominal $As_{55}S_{45}$ composition was prepared by nanomilling and tested as potential anticancer drug. Polyvinylpyrrolidone was used as steric stabilizer and inhibitor of agglomeration. Individual nanoparticles had average size of 192 nm (determined by photon cross-correlation spectroscopy) and had several times better dissolution ability in comparison with bulk $As_{55}S_{45}$. Effect of nanomilling is shown to be associated with formation of arsenic sulfide crystalline nanoparticles and free-volume entities located at the interface between nanoparticles and surrounding matrix as it follows from positron annihilation measurements. Cytotoxicity tests were performed using human melanoma cell line Bowes and confirmed high toxicity of the studied nanosuspension.

DOI: 10.12693/APhysPolA.126.902
PACS: 81.20.Wk, 81.05.Kf, 81.07.–b

1. Introduction

Arsenic compounds in the form of different available minerals, such as orpiment As_2S_3, realgar As_4S_4 or arsenolite As_2O_3, have a long history in different field of applications and their usage goes back to the ancient times [1]. They have been utilized for a long time in cosmetics, foods, glass, insecticides, pigments, and in medicine as well. Approximately 60 different arsenic preparations have been developed and used during the history [2]. Among arsenic sulfides, realgar and orpiment seem to be very effective in cancer treatment [3–5].

However, it is well known that the solubility of arsenic sulfides in water is extremely low. Poorly water-soluble drugs pose a great challenge in drug formulation development. Preparation of nanosuspensions seems to be appropriate solution. Nanosuspension is a sub-micron colloidal dispersion of particles which are stabilized by surfactants, polymers, or mixture of both [6]. Wet milling technique is one of the effective approaches to obtain such nanosuspensions [7]. During milling process, the particles break into smaller ones, and thus fresh surfaces are continuously generated [8].

In this work, the nanosuspension of melt-quenched arsenic sulfide of nominal $As_{55}S_{45}$ composition was prepared in a circulation mill in polyvinylpyrrolidone (PVP) and its properties, particle size distribution, dissolution and cytotoxicity effects were studied.

*corresponding author; e-mail: bujnakova@saske.sk

2. Materials and methods

The arsenic sulfide alloy of $As_{55}S_{45}$ composition was synthesized from elemental constituents, additionally purified with distillation (no worse than three nines) in evacuated (2×10^{-5} Pa) and sealed fused quartz ampoules [9]. The melt was kept at $\approx$ 1150 K and then quenched to room temperature in a slow *furnace-off* regime.

Crystalline state of the prepared alloy was controlled by X-ray diffraction (XRD) with Cu K_{α_1} radiation arranged in the optimized transmittance geometry in $2\theta-$step regime using automatic STOE STADI P diffractometer (STOE & Cie GmbH) supplied by linear position-precision detector. The XRD peak profiles were refined using WinPLOTR software, phase analysis being performed with the Rietveld refinement.

The nanosuspension was prepared in a laboratory circulation mill MiniCer (Netzsch). The 5 g of $As_{55}S_{45}$ alloy was milled in 300 mL of 0.5% PVP solution at 4000 rpm for 2 h. The mill was loaded to 85% with 0.6 mm ZrO_2 milling balls.

Fourier transform infrared (FTIR) spectroscopy measurements were conducted on Tensor 29 infrared spectrophotometer (Bruker) in the frequency range of 4000–400 cm^{-1} using KBr pellet method.

Free-volume distribution in the samples was characterized by annihilation lifetime (PAL) measurements. The PAL spectra were detected with fast-fast coincidence system ORTEC of 230 ps resolution at the temperature 22 °C and relative humidity 35%, provided by special climatic installation. Two identical parts of the same solid pellet were used to build *sandwich* geometry needed for PAL recording. Near 10^6 elementary annihilation events

were accumulated to determine the values of positron lifetimes τ and corresponding intensities I. All PAL spectra were decomposed into three components confirming trapping of positrons (in one preferential type of spatially-extended free-volume defects) and decaying of bounded electron–positron pairs (*ortho*-positronium *o*-Ps atoms). The source contribution was evidenced at the level of about 15%, which allowed practically full compensation of input from positrons annihilated in the Kapton® foil (τ = 0.372 ns). Average positron lifetime τ_{av}^{Σ}, was determined as a centre of mass of whole lifetime spectrum. Positron trapping modes (mean τ_{av} and defect-free bulk τ_{b} positron lifetimes, and positron trapping rate in defect τ_{d}) were parameterized in respect of known formalism of two-state positron trapping model [10]. Radius R of free-volume holes responsible for o-Ps decaying was calculated like in polymers using Tao–Eldrup equation [10].

The particle size distribution was measured by photon cross-correlation spectroscopy using a Nanophox particle sizer (Sympatec).

The conditions for dissolution tests were accepted from [11].

The cytotoxicity of $As_{55}S_{45}$ sample was determined by colony forming assay. The cells were seeded onto 6-well plates with a density of 60 cells per well and incubated overnight. The cells were then treated with samples at various concentrations (0.625, 1.25 and 2.5 μ g/ml). After incubation for 10 days, the colonies were stained with crystal violet and counted. The values of 50% inhibition concentration (IC_{50}) of each compound were determined from dose-effect relationship using the CompuSyn software (version 1.0.1; CompuSyn, Inc, Paramus).

3. Results and discussion

3.1. Input characterization of $As_{55}S_{45}$ alloy

The XRD analysis (Fig. 1) of the prepared alloy confirmed a mixture of three crystalline phases with remaining glassy-like material. Three different phases were detected, the room temperature dimorphite As_4S_3 modification (45%, space group *Pnma*), the high temperature dimorphite As_4S_3 modification of the same space group *Pnma* (22%), and the high temperature modification of β-realgar As_4S_4 (33%, space group $C2/c$). Low degree of crystallinity does not exclude small amount of amorphous phase present in the prepared alloy.

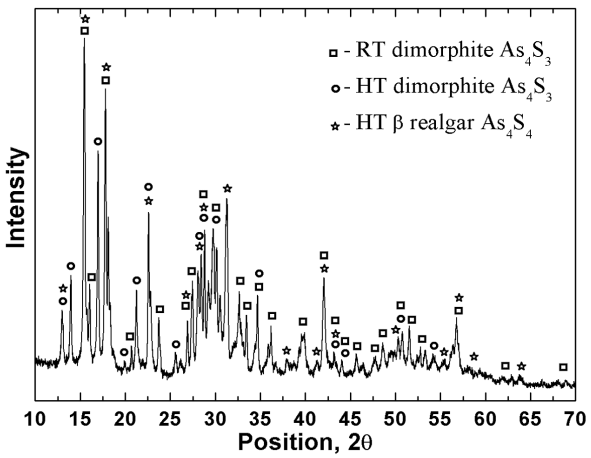

Fig. 1. XRD pattern of melt-quenched $As_{55}S_{45}$ alloy with theoretical XRD patterns for room temperature (RT) modification of dimorphite As_4S_3, high temperature (HT) modification of dimorphite As_4S_3 and high temperature (HT) modification of β-realgar As_4S_4.

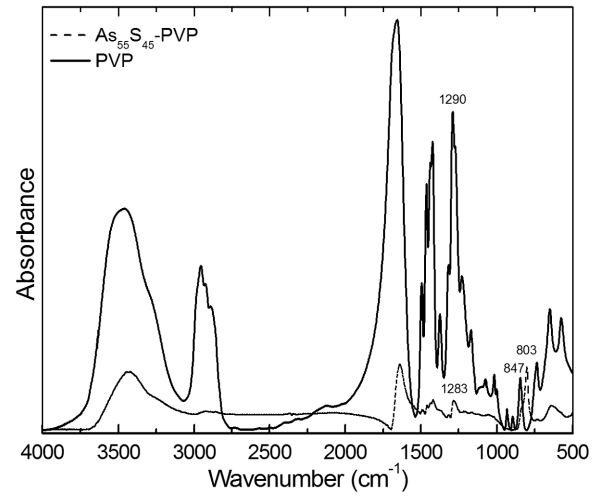

Fig. 2. FTIR spectra of pure PVP (solid line) and $As_{55}S_{45}$–PVP (dashed line).

3.2. Nanomilling

Five grams of the as-received powder of $As_{55}S_{45}$ alloy sample were subjected to the circulation milling process in 0.5% PVP aqueous solution. After 2 h of milling, the nanosuspension was filtered through 0.22 μm sterile filter. Both the liquid and the solid phases were used for further investigations.

3.3. Solid state characterization

3.3.1. FTIR spectroscopy

The FTIR spectroscopy was used to determine the possible chemical interaction between PVP and $As_{55}S_{45}$ nanoparticles during nanomilling. Comparing the spectrum (Fig. 2) of pure PVP with the spectrum of arsenic sulfide milled in PVP solution ($As_{55}S_{45}$–PVP), it was found a slight shift of the C–N stretching band from 1290 cm^{-1} to 1283 cm^{-1}, that could indicate on essential interaction between N from PVP and $As_{55}S_{45}$. The similar interaction was also found between PVP and silver nanoparticles [12]. Moreover, the C–C ring stretching band moved from 847 cm^{-1} to 803 cm^{-1} resulting in the dislocation of the aliphatic chain in PVP from its original position due to $As_{55}S_{45}$–PVP interaction. The lower intensity of FTIR spectrum of $As_{55}S_{45}$–PVP nanosuspension in comparison with pure PVP is possibly caused by influence of nanomilling.

3.3.2. PALS

Raw PAL spectra of pure PVP and $As_{55}S_{45}$–PVP are shown in Fig. 3, numerical characteristics of the crresponding trapping modes being gathered in Table I.

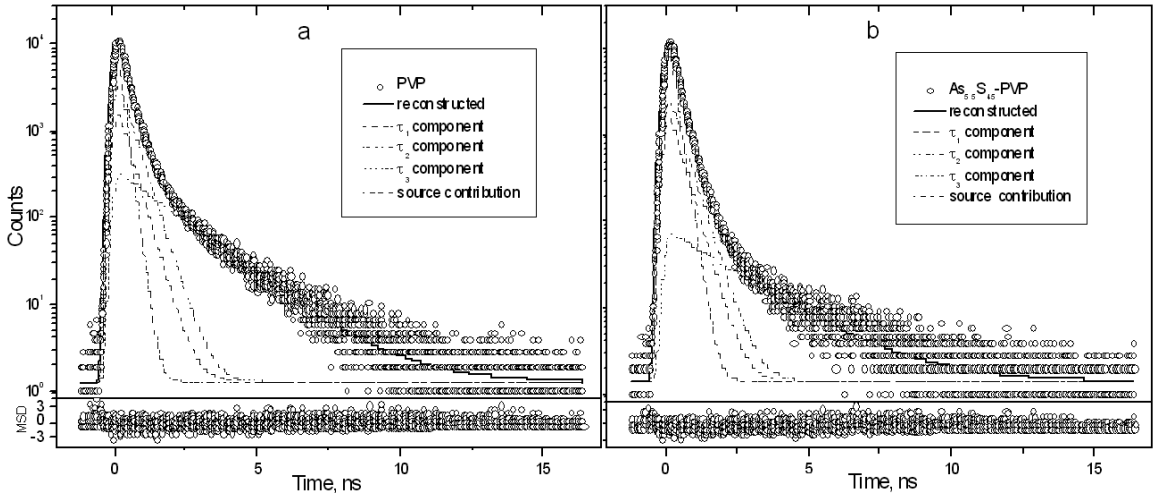

Fig. 3. Raw PAL spectra of (a) pure PVP and (b) $As_{55}S_{45}$–PVP reconstructed from three-component decomposition procedure at the background of source contribution (bottom insets show statistical scatter of variance).

TABLE I

Fitting parameters, positron trapping and o-Ps decaying modes describing positron annihilation in $As_{55}S_{45}$–PVP.

Sample	Decompo-sition	τ_1 [ns]	I_1 [%]	τ_2 [ns]	I_2 [%]	τ_3 [ns]	I_3 [%]	$\tau_{av.}^{\Sigma}$ [ns]	$\tau_{av.}$ [ns]	τ_b [ns]	κ_d $[ns]^{-1}$	τ_2/τ_b	R [nm]
PVP	1	0.196	62.5	0.472	25.6	1.867	11.9	0.466	0.276	0.237	0.867	2.00	0.276
$As_{55}S_{45}$-PVP	1	0.20	71.3	0.426	26.0	2.215	2.7	0.313	0.26	0.233	0.709	1.83	0.305
	2	0.198	67.9	0.378	31.5	5.028	0.6	0.282	0.255	0.233	0.770	1.62	0.484

TABLE II

Flow cytometry analysis of Bowes cell line treated with ATO and $As_{55}S_{45}$ at different As concentrations for 24–72 h. L — live, A — apoptotic, N — necrotic cells.

BOWES	24 h			48 h			72 h		
	L [%]	A [%]	N [%]	L [%]	A [%]	N [%]	L [%]	A [%]	N [%]
Control	91.8	3.4	3.2	94.9	2.1	2.5	86.4	4.1	8.5
ATO (0.625 μg/mL)	86.5	5.3	6.5	59.7	16.4	23.3	28	17	54.5
$As_{55}S_{45}$ (0.625 μg/mL)	69.7	14.3	13.7	48.3	12.2	44.1	3.5	15	81.3
ATO (1.25 μg/mL)	75.9	11.6	10.5	36.9	14.8	48	1.3	13.6	85
$As_{55}S_{45}$ (1.25 μg/mL)	55.9	16.2	27.6	9.1	13.4	77.5	0.6	18.3	81.1
ATO (2.5 μg/mL)	61	16	22	11.9	11.2	76.7	0.5	15.9	83.5
$As_{55}S_{45}$ (2.5 μg/mL)	15.9	14.7	69.3	2.5	13.8	83.7	0.4	22.3	77.3

Since expected channels of positron annihilation (free-volume sub-nanometer voids) in such structurally complicated composites with embedded nanoparticles are modified with a necessity by all possible components (including PVP remainders, nanocrystalline particles, amorphous intergrain inclusions and grain boundaries, etc.), the PAL data for pure PVP were also given in Table I for comparison. These spectra for pure PVP and $As_{55}S_{45}$–PVP were decomposed into three components under fixed contribution from source (decomposition procedure 1). We showed also the results of PAL spectra deconvolution in $As_{55}S_{45}$–PVP corrected with additional input from

pure PVP (decomposition procedure 2). In this case, the o-Ps decaying is enormously distorted by over-estimated input from PVP sub-system (tending I_3 intensity towards 0), but positron trapping modes as affected directly by sites appearing due to nanoparticles themselves are refined better.

Strong influence of *o*-Ps decaying modes due to PVP inclusions in nanocomposite samples is really essential due to the character value of long-lived lifetime $\tau_3 \approx 1.9$ ns and high corresponding intensity $I_3 \approx 12\%$ proper to this polymer. Formation of *o*-Ps is strongly inhibited by presence of arsenic sulphide nanoparticles as it follows from the drastic decrease in I_3 value to 2.7% in $As_{55}S_{45}$–PVP. This difference is evident from even visual inspection of both spectra in Fig. 3. $As_{55}S_{45}$–PVP sample demonstrate faster decaying as compared with pure PVP sample, probably due to additional channel of positron trapping in nanostructured grains. The mean radius of free-volume voids (R) increased from ≈ 0.276 to ≈ 0.305 nm and it is in contrast to [13], where its decrease was observed in $NiFe_2O_4$ nanoparticles embedded in SiO_2 matrix. This testifies that nanocomposite structure results from mixing of ingredients (arsenic sulfide polymorphs in $As_{55}S_{45}$ alloy) in PVP environment and appeared positron traps are voids at the interfaces between separate nanoparticles surrounded by PVP. Assuming this channel as general input to the decomposed PAL spectra (decomposition procedure 2), we obtained the characteristic lifetime for these traps close to ≈ 0.38 ns and defect-free bulk lifetime in the nanoparticle agglomerates $\tau_b = 0.233$ ns. This last value is very close to $\tau_b = 0.242$ ns, the value predicted for orthorhombic arsenic sulfide in respect to earlier DFT calculations [14].

3.3.3. Dissolution

The low solubility of arsenic sulfides is well-known and intensification factors to avoid this shortcoming are evidently needed. The dissolution of the solid phase of the as-received and milled $As_{55}S_{45}$ samples in a simulated gastric (SGF) and intestinal fluid (SIF) was tested (pH = 1.3 and 6.5, respectively). In the as-received sample, the amount of dissolved arsenic after 240 min of leaching in SGF + SIF was only 0.4%. On the other hand, nanonization in circulation mill leads to sharp increase in As dissolution up to 10% (Fig. 4). Nanoparticles possess an increased dissolution rate due to their large surface-to-volume ratio, but also show an increased saturation solubility [15]. Moreover, the observed increase in the reactivity correlate well with detection of additional positron trapping sites related to nanoparticle–PVP interface as it follows from PAL experiments above.

3.4. Biological activity

The biological activity of the prepared nanosuspension having the particle size distribution given in Fig. 5a was tested. This study was mainly designed to determine whether $As_{55}S_{45}$ nanosuspension induces cytotoxicity. As the example, the Bowes human melanoma cell line was selected. The results (Table II) were compared with

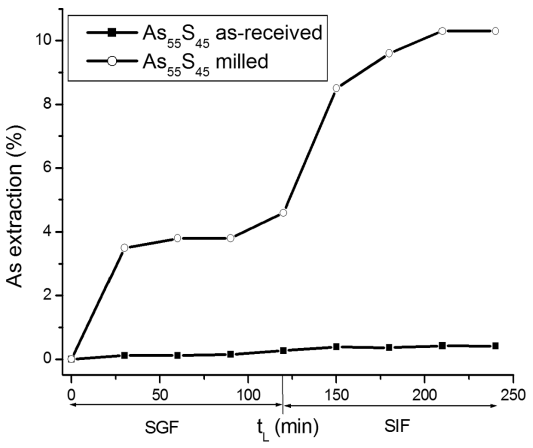

Fig. 4. Arsenic extraction for as-received and milled $As_{55}S_{45}$ samples leached in simulated gastric and intestinal fluids (SGF and SIF, respectively); leaching time, $t_L = 240$ min, leaching temperature = 36.5 °C.

the arsenic trioxide, As_2O_3 or ATO, whose cytotoxicity effect on various cell lines is well documented [16, 17]. In a comparison with the non-treated control cells, when the Bowes cells were incubated with 0.625 μg/mL of As from ATO or $As_{55}S_{45}$ for 24 h, it can be seen that the portion of live cells (L) decreased in both of cases (from 91.8% to 86.5% and 69.7%, respectively). On the other hand, the amount of apoptotic (A) and necrotic (N) cells increased (from 3.4% to 5.3% and 14.3% for A cells and from 3.2% to 6.5% and 13.7% for N cells). When ATO and $As_{55}S_{45}$ compared, the higher toxicity was obtained in latter compound. With the increase of incubation time, the increase of N cells was observed mostly. In the case of $As_{55}S_{45}$, 81.3% of cells were necrotic after 72 h of incubation. It confirmed a high toxicity of the sample. The changes are more visible, when the higher arsenic concentrations (1.25 and 2.5 μg/mL) were applied — the amount of A and N cells increased more.

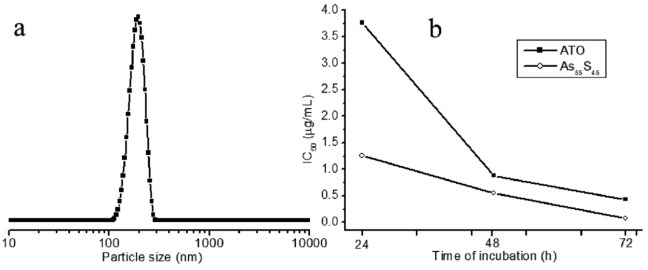

Fig. 5. (a) Particle size distribution of $As_{55}S_{45}$ nanosuspension and (b) IC_{50} for Bowes cell line treated with ATO and $As_{55}S_{45}$.

The half maximal inhibitory concentration or IC_{50} value was depicted in Fig. 5b. In this case, it is a concentration of arsenic at which 50% of cancer cell population is inhibited. When compared IC_{50} curves for ATO and

$As_{55}S_{45}$, it can be seen that the prepared arsenic sulfide compound is more toxic, because cancer cells are inhibited at lower arsenic concentrations. Moreover, the decrease of IC_{50} value with the time of incubation for $As_{55}S_{45}$ has linear character.

4. Conclusions

In this work, the arsenic sulfide $As_{55}S_{45}$ nanosuspension was prepared by nanomilling. This process is accompanied by reconstruction of the existing free-volume voids trapping positrons as it follows from PAL study. The dissolution percentage of arsenic from the prepared sample increased from 0.4% to 10%. The detected anticancer effect on Bowes human melanoma cell line confirmed the high toxicity of the studied material. To our best of knowledge no previous works have been reported on anticancer effect of $As_{55}S_{45}$ compound.

Acknowledgments

This work was supported by the projects APVV-0189-10, VEGA 2/0027/14, VEGA 2/0064/14 and bilateral SAS-NSC JRP 2010/03 and APVV SK-UA-2013-0003. Assistance in the XRD measurements by Dr. Pavlo Demchenko (Inorganic Chemistry Dpt. of the Ivan Franko National University of Lviv, Ukraine) is gratefully acknowledged.

References

[1] R. Bentley, T.G. Chasteen, *Chem. Educator* **7**, 51 (2002).

[2] W.H. Miller, Jr., H.M. Schipper, J.S. Lee, J. Singer, S. Waxman, *Cancer Res.* **62**, 3893 (2002).

[3] J.-Z. Wu, P.C. Ho, *Eur. J. Pharm. Sci.* **29**, 35 (2006).

[4] P. Baláž, J. Sedlák, M. Pastorek, D. Cholujová, K. Vignarooban, S. Bhosle, P. Boolchand, Z. Bujňáková, E. Dutková, O. Kartachova, B. Stalder, *J. Nano Res.* **18-19**, 149 (2012).

[5] P.J. Dilda, P.J. Hogg, *Cancer Treat. Rev.* **33**, 542 (2007).

[6] B.E. Rabinov, *Nat. Rev. Drug Discov.* **3**, 785 (2004).

[7] E. Merisko-Liversidge, G.G. Liversidge, *Adv. Drug Deliver. Rev.* **63**, 427 (2011).

[8] P. Baláž, *Mechanochemistry in Nanoscience and Mineral Enginering*, Springer Verlag, Berlin, Heidelberg 2008.

[9] A. Feltz, *Amorphous Inorganic Materials and Glasses*, VCH Publishers, New York 1993.

[10] K. Krause-Rehberg, H.S. Leipner, *Positron annihilation in semiconductors. Defect studies.* Springer, Berlin, Heidelberg 1999.

[11] D.D. Hörter, J.B. Dressman, *Adv. Drug Deliver. Rev.* **46**, 75 (2001).

[12] X.H. Wang, X. Qiao, J. Chen, X. Wang, S. Ding, *Mater. Chem. Phys.* **94**, 449 (2005).

[13] S. Mitra, K. Mandal, S. Sinha, P.M.G. Nambissan, S. Kumar, *J. Phys. D, Appl. Phys.* **39**, 4228 (2006).

[14] K.O. Jensen, P.S. Salmon, I.T. Penfold, P.G. Coleman, *J. Non-Cryst. Solids* **170**, 57 (1994).

[15] L. Wu, J. Zhang, W. Watanabe, *Adv. Drug Deliver. Rev.* **63**, 456 (2011).

[16] Y.J. Chen, Y.P. Lin, L.P. Chow, T.C. Lee, *Proteomics* **11**, 4331 (2011).

[17] C.W. Chien, J.H. Yao, S.Y. Chang, P.C. Lee, T.C. Lee, *Toxicol. Appl. Pharmacol.* **257**, 59 (2011).